

QUANTITATIVE ANALYSIS OF OBSERVED SEISMIC
STRAINS IN UNDERGROUND STRUCTURES *

by

Masahiro NAKAMURA^{I)}, Tsuneo KATAYAMA^{II)}
and Keizaburo KUBO^{III)}

SYNOPSIS

The observed seismic strains of several types of underground structures were quantitatively analyzed. A total of 123 seismic records obtained during 91 earthquakes in seven buried pipelines, three submerged tunnels, two embedded tanks and a rock tunnel were analyzed. The general levels of seismic strains were found to differ according to the types of underground structures. On average, by assuming the seismic strain of buried pipelines to be unity, those of submerged tunnels and embedded tanks were found to be about 0.39 and 0.14, respectively. The seismic strain of buried pipelines was found more strongly correlated with the peak ground velocity than with the ground acceleration. The measured strains were then compared with the calculated strains obtained by the Technical Guidance for Petroleum Pipeline. The calculated strains were found to generally give much higher values than the measured strains, indicating that the present Technical Guidance may be too conservative to estimate the seismic pipe strains.

INTRODUCTION

In recent years, the roles of underground structures, such as buried pipelines, submerged tunnels, embedded tanks and rock tunnels, are becoming increasingly more important in the civil engineering construction. Past studies have shown that the dynamic responses of these structures during earthquakes are greatly influenced by the behavior of the surrounding soil[1-3]. By reflecting the abovementioned finding, the response-displacement method is

* Presented at the January 14-16, 1981, Review Meeting of the U.S.-Japan Cooperative Research on "Seismic Risk Analysis and Its Application to Reliability-Based Design of Lifeline Systems" held at Honolulu, Hawaii.

I) Visiting Research Personnel(Technical Research Laboratory, Fujita Co., Ltd.), II) Associate Professor, and III) Professor, Institute of Industrial Science, University of Tokyo.

widely used in Japan for the earthquake resistant design of these structures[4-6]. However, the distribution of ground displacement during an earthquake, namely the seismic strain in the ground, has not been well understood today. Therefore, observed data of ground strain during earthquakes supply very important information for the design of underground structures. Although the direct measurement of the seismic ground strain is generally difficult, it has been conclusively shown that the buried pipe strains may in most cases be considered to represent the soil strains during an earthquake[1].

In this paper, the seismic strains produced in underground structures are quantitatively investigated by using the 123 data recorded in Japan. They include the data in seven buried pipelines [7-16], three submerged tunnels[2,17-21], two embedded tanks[3,22, 23] and one rock tunnel[24]. In the latter part of the paper, the strains calculated by the method specified in the Technical Guidance for Petroleum Pipeline[4], which is frequently used for the earthquake resistant design of buried pipelines in Japan, are compared with the observed data.

OBSERVED SEISMIC STRAINS IN UNDERGROUND STRUCTURES

OBSERVATION SITES AND EARTHQUAKE RECORDS: The records of the 91 earthquake events from 1970 to 1980 observed at 13 sites for the four types of underground structures were investigated in this study. Table 1 shows the list of the observation sites, types of structures and their relevant properties. The epicenters, depths and magnitudes of the 91 earthquakes are summarized in Table 2. The first columns of Tables 1 and 2 assign reference numbers for all the observation sites and earthquakes, respectively. By using these reference numbers, the complete information of the 123 data are summarized in Table 3. There are 60, 48, 9 and 6 observations for buried pipelines, submerged tunnels, embedded tanks and a rock tunnel, respectively. The x and y axes were taken in the horizontal plane. The x axis was taken along the longitudinal direction of a structure for pipes and tunnels and the y axis perpendicular to the x axis. The z axis was taken along the vertical direction. STRAIN 1 in Table 3 indicates the longitudinal axial strain ϵ_L for linear structures and the horizontal circumferential strain for embedded tanks. STRAIN 2 indicates the circumferential strain for buried pipelines, the bending strain for submerged tunnels and the vertical axial strain for embedded tanks.

CHARACTERISTICS OF OBSERVED SEISMIC STRAINS: Figure 1 shows the cumulative frequency distributions of observed strains ϵ for the four different types of structures. It is clearly seen that the observed strains are the smallest for the rock tunnel and the largest for the buried pipelines.

To examine the effect of acceleration level, the cumulative

frequency distributions of ϵ/a are plotted in Fig. 2, where a is the measured peak acceleration. When the strains are normalized by the peak accelerations, the curves of buried pipelines and submerged tunnels are found to exhibit almost similar tendencies.

Figure 3 is shown to illustrate the effect of ground conditions on seismic strains. For this purpose, the measured strain was normalized by the product of the peak acceleration a and the natural period of the ground T in the form of $\epsilon/(a \cdot T/2\pi)$. Since the quantity $a \cdot T/2\pi$ in the denominator has the dimension of velocity, the ratio $\epsilon/(a \cdot T/2\pi)$ may be considered as the strain per unit ground velocity. The information contained in Fig. 3 is considered more general than those in Figs. 1 and 2 because the strain is normalized by the site factor T as well as by the ground shaking intensity a . The seismic strain generally increases in the following order: embedded tanks, rock tunnels, submerged tunnels and buried pipelines. While the rock tunnel gave the smallest strain in Fig. 1, the smallest strain in Fig. 3 corresponds to the embedded tank. This change has probably resulted from the fact that, while the strain in the rock tunnel is almost the same as that in the surrounding rock, the strain in the embedded tank is considerably smaller than that in the surrounding ground[3]. At the 50%-level of the cumulative frequency distribution, the ratios among the strains per unit velocity of pipeline, submerged tunnel and embedded tank are 1:0.39:0.14. Although both pipelines and submerged tunnels are linear structures, the strain levels produced during earthquakes are quite different. This is probably due to the difference between their cross-sectional areas.

In Fig. 4, the buried pipelines are divided into two groups according to their diameters, namely $D < 1000$ mm and $D > 1000$ mm. However, the two curves corresponding to these two groups do not show any significant difference. This seems to indicate that the effect of pipe size is not significant within the diameter range between 160 mm and 1800 mm. Note, however, that this statement cannot be conclusive because of the insufficient number of data available at present.

Measured "axial" strains ϵ_L of pipes and tunnels are shown in Fig. 5 for the four different groups of earthquake magnitudes ($M > 7$, $7 > M > 6$, $6 > M > 5$ and $5 > M$) plotted against the epicentral distance. It is interesting to notice that the slope of the regression line for $M > 7$ is smaller than those for $7 > M > 6$ and $6 > M > 5$. This seems to indicate that the strains caused by large earthquakes do not decrease rapidly with the increase in epicentral distance. The regression equations and some relevant quantities are also shown in Fig. 5. Since the effect of ground condition is not considered, the coefficients of correlation are not high.

All the regression equations obtained in this study are summarized in Table 4.

SEISMIC STRAINS IN BURIED PIPELINES

In most cases it is difficult to directly measure the strains in the ground caused by an earthquake. However, past studies have conclusively shown that the strains produced in pipelines during an earthquake are almost the same as those of the surrounding ground[1]. In fact, it is always more practical to estimate the approximate soil strains in the surrounding ground from the measured pipe strains. In this section the observed strains in the buried pipelines during earthquakes are investigated in detail.

The observed "axial" pipe strains ϵ_L are plotted in Fig. 6 against the epicentral distance for the earthquakes with magnitudes equal to or greater than 7. Since the effect of ground condition is not considered, the coefficient of correlation is low ($\gamma=-0.474$). Generally, the observed pipe strains in the soft ground with a longer natural period is much higher than those in a harder ground with a shorter natural period. Hence, the pipe strain was normalized by the corresponding natural period of ground. The results are shown in Fig. 7, which shows a considerably higher value of the coefficient of correlation ($\gamma=-0.679$).

The axial pipe strains ϵ_L are plotted against the peak accelerations α_x , α_y and α_z in Figs. 8, 9 and 10, respectively. The correlations between accelerations and axial strains in these figures are relatively high with the coefficients of correlation γ being 0.756, 0.716 and 0.791 for α_x , α_y and α_z , respectively. The correlation between ϵ_L and α_x is again examined in Fig. 11 for the two groups of data classified according to the epicentral distance Δ . The observed data were divided into two groups with $\Delta < 150$ km and $\Delta \geq 150$ km. It can be easily seen from Fig. 11 that the earthquakes with longer epicentral distances tend to produce higher axial pipe strains for the same acceleration level than those with shorter distances do. This tendency is also apparent in Figs. 9 and 10.

The axial pipe strains are plotted again in Fig. 12 against $\alpha_x \cdot T/2\pi$ in order to approximately take into account the effect of ground condition. The coefficients of correlation γ are found to be much higher than those obtained in Fig. 8, indicating that the axial pipe strains are more strongly correlated to the ground velocity than to the ground acceleration. The coefficient of correlation γ is as high as 0.944 for $M > 7$. As can be seen from Table 3, there are 17 observed strain data for which the ground velocities were also measured. Figure 13 shows the plot of these 17 data against the measured longitudinal peak velocity v_x . The high value of $\gamma=0.898$ clearly indicates the strong correlation between the axial pipe strain and the velocity.

DATA FROM THE 1978 MIYAGI-KEN-OKI EARTHQUAKE

During the 1978 Miyagi-ken-oki earthquake ($M=7.4$), records were

obtained at 8 sites out of the 13 listed in Table 1. At one site, the maximum recorded pipe strain reached 299×10^{-6} .

The measured axial strains of linear structures (buried pipelines and submerged tunnels) are shown in Fig. 14 plotted against the measured peak acceleration a_x . The regression line in Fig. 14 is that obtained from the previous analysis ($M > 7$ in Fig. 8). The regression line obtained by using the peak acceleration as the variable is found to fail to explain the two points at the higher acceleration level.

In Fig. 15, the axial strain ϵ_L is plotted against the parameter ($a_x \cdot T / 2\pi$) as was done in Fig. 12. The regression line previously obtained in Fig. 12 for $M > 7$ earthquakes now shows a much better agreement with the data especially at the higher strain levels. As can be seen from Tables 1 and 3, the largest observed strain of 299×10^{-6} was obtained for $a_x = 125$ gal at the site with $T = 1.3$ sec. The calculated strain for these a_x and T values is 180×10^{-6} which is about 60% of the observed value. Although the calculated strain is still small, the agreement in Fig. 15 is considered reasonable.

Figure 16 shows the relations between ϵ_L and T by using the regression line for $M > 7$ obtained in Fig. 12 for several different values of the peak acceleration. By using this figure, for $a_x = 500$ gal and $T = 2$ sec, for example, ϵ_L may be easily estimated to be about 1100×10^{-6} . Note, however, that the lines in Fig. 16 are still very tentative because of the lack of observed data.

SEISMIC PIPE STRAINS CALCULATED BY THE TECHNICAL GUIDANCE FOR PETROLEUM PIPELINE

In Japan, the earthquake resistant design of buried pipelines is often performed according to the Technical Guidance for Petroleum Pipeline [4, 25, 26]. A buried pipeline in the x direction as shown in Fig. 17 is considered. A shear wave with a wave length L and a displacement amplitude U is assumed to propagate in the direction of the x' axis, which makes an angle of ϕ with the pipe axis. The amplitude U is decomposed into two components U_L and U_B , where U_L is the component in the pipe direction (x -axis) and U_B is the component perpendicular to the pipe direction.

$$U_L = U \cdot \sin\phi \cdot \sin\left[\frac{2\pi \cdot \cos\phi}{L} x\right] \quad (1)$$

$$U_B = U \cdot \cos\phi \cdot \sin\left[\frac{2\pi \cdot \cos\phi}{L} x\right] \quad (2)$$

The longitudinal axial strain e_L and the transverse bending strain e_B of the virtual soil pipeline are obtained by

$$e_L = \frac{\partial U_L}{\partial x} = \frac{2\pi \cdot U}{L} \sin\phi \cdot \cos\phi \cdot \cos\left[\frac{2\pi \cdot \cos\phi}{L} x\right] \quad (3)$$

$$e_B = \frac{D/2}{\rho} = \frac{2\pi^2 \cdot D \cdot U}{L^2} \cos^3 \phi \cdot \sin\left[\frac{2\pi \cdot \cos \phi}{L} x\right] \quad (4)$$

where D is the pipe diameter, and the radius of curvature ρ of pipe is obtained from

$$\frac{1}{\rho} = \frac{\partial^2 U_B}{\partial x^2} \quad (5)$$

By putting $\cos\left[\frac{2\pi \cdot \cos \phi}{L} x\right]$ and $\sin\left[\frac{2\pi \cdot \cos \phi}{L} x\right]$ equal to unity in Eqs. (3) and (4), respectively, it is found

$$e_L = \frac{2\pi \cdot U}{L} \sin \phi \cdot \cos \phi \quad (6)$$

$$e_B = \frac{2\pi^2 \cdot D \cdot U}{L^2} \cos^3 \phi \quad (7)$$

The maximum values of e_L and e_B denoted by e_{Lmax} and e_{Bmax} , respectively, become

$$e_{Lmax} = \frac{\pi \cdot U}{L} \quad \left(\phi = \frac{\pi}{4}\right) \quad (8)$$

$$e_{Bmax} = \frac{2\pi^2 \cdot D \cdot U}{L^2} \quad (\phi = 0) \quad (9)$$

The factors of transmission to convert these ground strains to the pipeline strains are determined by considering the physical properties of the pipeline, the surrounding soil and the propagating wave. The factors α_1 and α_2 for the longitudinal axial and the transverse bending strain, respectively, are

$$\alpha_1 = \frac{1}{1 + \frac{2\pi^2 \cdot E \cdot S}{L^2 \cdot K_1}} \quad (10)$$

$$\alpha_2 = \frac{1}{1 + \frac{16\pi^4 \cdot E \cdot I}{L^4 \cdot K_2}} \quad (11)$$

where

E = Young's modulus of pipe

S = Cross-sectional area of pipe

I = Moment of inertia of pipe

K_1 = Force per unit surface area of pipe that produces a unit of relative axial displacement between pipe and soil

K_2 = Force per unit surface area of pipe that produces a unit of relative lateral displacement between pipe and soil

Generally speaking, the values of α_1 and α_2 are almost equal to 1 for most practical cases. Therefore, the strains produced in a buried pipeline may be assumed to be approximately equal to the strains of the ground.

According to the Technical Guidance, the design strain e_T is obtained by

$$\begin{aligned} e_T &= \sqrt{2(1^2 + 0.75^2)(\alpha_1 \cdot e_{Lmax})^2 + (\alpha_2 \cdot e_{Bmax})^2} \\ &= \sqrt{3.12(\alpha_1 \cdot e_{Lmax})^2 + (\alpha_2 \cdot e_{Bmax})^2} \end{aligned} \quad (12)$$

where the pipe is assumed to be simultaneously subjected to five incident shear waves.

The displacement amplitude U appearing in the previous equations is calculated by

$$U = \frac{2}{\pi^2} \cdot T \cdot S_V \cdot K_{Oh} \quad (13)$$

where

T = Natural period of ground

K_{Oh} = Seismic coefficient to be assumed at the base ground

S_V = Velocity response spectral amplitude of the ground motion with a peak acceleration of 1g (g = acceleration of gravity)

The natural period of ground T is calculated by

$$T = 4 \sum \frac{H_i}{V_{si}} \quad (14)$$

where

H_i = Thickness of the i -th layer

V_{si} = Shear wave velocity of the i -th layer

The velocity response spectrum (S_V) to be used in Eq.(13) is shown in Fig. 18.

COMPARISONS OF CALCULATED STRAINS AND OBSERVED STRAINS

According to the flow chart shown in Fig. 19, the strains calculated by the Technical Guidance were compared with the observed buried pipe strains ε_L . Since the strains are first calculated by assuming an input acceleration of $A=U(2\pi/T)^2$, the values e_{Lmax} and e_T must be multiplied by a factor $C=\alpha_x/A$ before they are compared with the observed strains. The symbols e_{CG} , e_{CL} and e_{CT} used in the following part are $C \cdot e_{Lmax}$, $C \cdot \alpha_1 \cdot e_{Lmax}$ and $C \cdot e_T$, respectively.

The cumulative frequency distributions of e_{CG}/ε_L , e_{CL}/ε_L and e_{CT}/ε_L are shown in Fig. 20. For the 50%-level on the vertical scale the values of e_{CL}/ε_L , e_{CG}/ε_L and e_{CT}/ε_L are 2.5, 2.7 and 4.3, respectively. It is interesting to note that e_T obtained from the Technical Guidance is 4.3 times larger than observed value.

Figure 20 also shows the cumulative frequency distribution curve e_p/ε_L , in which the calculated strain e_p was obtained by the method proposed by the authors[27,28,29]. The value of e_p/ε_L at the 50%-level is approximately 1.5, indicating that the calculated strain e_p is much closer to the observed value than the strains by the Technical Guidance are.

The greatest pipe strain (299×10^{-6}) during the Miyagi-ken-oki earthquake was observed at the Shimonaga site as shown in Table 1. The strains calculated by the method of the Technical Guidance (e_{CL} , e_{CG} and e_{CT}) and the authors' method (e_p) as well as observed data during several earthquakes are shown in Fig. 21. The Shimonaga site is covered with a 40 m soft surface layer with an average N-value of 7[11]. This surface layer is composed of peat, soft sandy and silty soils.

All the calculated strains are larger than the observed ones. Moreover, the values e_{CT} calculated by the method of the Technical Guidance show the greatest difference, while the values e_p calculated by the authors' method show the smallest difference. The observed data (earthquake magnitudes, pipe strains and peak accelerations) and the ratios e_p/ε_L , e_{CL}/ε_L , e_{CG}/ε_L and e_{CT}/ε_L are shown in Table 5. It seems interesting to note that as the magnitudes of earthquakes increase the ratios between the calculated and the measured strain decrease. For example, the ratios e_{CT}/ε_L for $M=5.8$ and 7.4 are 22.8 and 3, respectively. In any case, it is important to accumulate more observed data, especially those produced by large magnitude earthquakes in order to make a more reliable estimate of the seismic strains of buried pipelines.

CONCLUSIONS

In this paper, seismic strains observed in several kinds of underground structures (buried pipelines, submerged tunnels, embedded tanks and a rock tunnel) were investigated, and the strains calculated by the Technical Guidance for Petroleum Pipeline in Japan

were compared with the observed strains. Major points of interest found from the study reported in this paper are summarized below.

- (1) The level of the normalized seismic strains $\epsilon/(\alpha \cdot T/2\pi)$ generally differ according to the different types of underground structures. Supposing that the strain in a buried pipeline is 1, the strains in a submerged tunnel and an embedded tank are 0.39 and 0.14, respectively.
- (2) The decrease of the seismic strain of buried structures with distance is slower for large magnitude earthquakes than for smaller earthquakes.
- (3) For the same level of the peak acceleration (or velocity), the seismic strain increases with the earthquake magnitude and the epicentral distance.
- (4) The axial strain ϵ_L in a buried pipeline is more strongly correlated with the peak ground velocity v_x or $(\alpha_x \cdot T/2\pi)$ than with the peak ground acceleration α_x . The regression line obtained for $M > 7$ earthquakes was

$$\log \epsilon_L = 1.02 \cdot \log \frac{\alpha_x \cdot T}{2\pi} + 0.804$$

with a surprisingly high value of the coefficient of correlation of 0.94.

- (5) The compound axial strain e_{CT} calculated by the Technical Guidance for Petroleum Pipeline is, on average, 4 times greater than the observed strain.

ACKNOWLEDGMENTS

The authors express special appreciation to the following persons for providing the valuable information on the results of earthquake observations of buried structures.

T. Ukaji, K. Tsukamoto, K. Koyama (Tokyo Gas Co.); S. Hojo, T. Iwamoto, N. Wakai (Kubota Ironworks, Ltd.); M. Nishizuka, M. Tomii (Kanagawa Water Supply Authority); J. Tsujimoto, F. Okuma (Nippon Steel Corp.); T. Fujisawa (Ministry of Transport); H. Oishi (Nippon Kokan Corp.).

REFERENCES

- (1) A. Sakurai, T. Takahashi, H. Tsutumi, H. Yajima, T. Noguchi and T. Iwakata (1967), "Dynamic Stresses of Underground Pipe-

- lines during Earthquakes (A Study Based on the Observed Records in the Matsushiro Earthquakes) (in Japanese)", Report No. 67058, Technical Laboratory, Central Research Institute of Electric Power Industry.
- (2) C. Tamura, S. Okamoto and M. Hamada (1975), "Dynamic Behavior of a Submerged Tunnel during Earthquakes", Report of the Institute of Industrial Science, the University of Tokyo, Vol. 24, No. 5.
 - (3) M. Hamada (1979), "Basic Investigation on Dynamic Behavior of a Large-Scale Embedded Tank during Earthquakes (in Japanese)", Thesis to University of Tokyo.
 - (4) Ministerial Notification on Details of Engineering Requirements for Oil Pipeline Enterprise, Notification No. 1 of Ministry of International Trade and Industry, Ministry of Transport, Ministry of Construction and Ministry of Autonomy, 1973 (in Japanese).
 - (5) Earthquake Resistant Design Guidance for Submerged Tunnel (Proposal), JSCE, 1975 (in Japanese).
 - (6) Technical Guidance for Underground Storage Facilities (Proposal), JSCE, 1980 (in Japanese).
 - (7) N. Nishio, T. Ukaji and K. Tsukamoto (1978), "Observation of Dynamic Behavior of Underground Pipelines during Earthquakes (in Japanese)", Proceedings of the 5th Japan Earthquake Engineering Symposium.
 - (8) N. Nishio et al. (1977), "Study on Stresses of Buried Pipeline during Earthquakes (No. 1)", Report of Technical Laboratory, Tokyo Gas Co., Vol. 22.
 - (9) N. Nishio, K. Yoneyama, T. Ukaji, K. Tsukamoto and J. Hamura (1979), "Study on Stresses of Buried Pipeline during Earthquake (No. 2) (in Japanese)", Report of Technical Laboratory, Tokyo Gas Co., Vol. 24.
 - (10) M. Kogarumai, S. Hojo and T. Iwamoto (1978), "Observations of Dynamic Behavior of Anti-Earthquake Ductile Pipes in Water-Main for Supply to Water Purification Yard at Hakusan, Hachinohe City during Earthquake (in Japanese)", Proceedings of the 5th Japan Earthquake Engineering Symposium.
 - (11) M. Kogarumai, S. Hojo and N. Wakai (1979), "Observations of Dynamic Behavior of Anti-Earthquake Ductile Pipes at Shimonaga, Hachinohe City during Earthquake (in Japanese)", Proceedings of the 15th Earthquake Engineering Seminar, JSCE.
 - (12) S. Hojo and T. Iwamoto (1979), "Observation of Dynamic Behavior of Anti-Earthquake Ductile Pipes of Type S at Hachinohe City during Earthquake (in Japanese)", Report of Ductile Steel Pipe, Vol. 26.
 - (13) J. Miyauchi and J. Tsujimoto (1980), "Dynamic Behavior of Pipeline during the Miyagi-ken-okii Earthquake in 1978", the 7th WCEE.
 - (14) M. Miyajima, J. Miyauchi, K. Shirakawa and Y. Aono (1976), "An Example of Seismic Design and Earthquake Response Measurement of Buried Pipeline", U.S.-Japan Seminar on Earthquake

- Engineering Research with Emphasis on Lifeline Systems.
- (15) H. Fujioka, M. Nishizuka and M. Takahashi (1980), "Observation of Dynamic Behavior of Buried Steel Pipeline during Earthquakes and Earthquake Resistant Design (I) (in Japanese)", JWWA, Vol. 550.
 - (16) H. Fujioka, M. Nishizuka and M. Takahashi (1980), "Observation of Dynamic Behavior of Buried Steel Pipeline during Earthquakes and Earthquake Resistant Design (II) (in Japanese)", JWWA, Vol. 552.
 - (17) C. Tamura, S. Okamoto and K. Kato (1976), "Strains of Submerged Tunnel during Earthquakes (in Japanese)", Proceedings of the 14th Earthquake Engineering Seminar, JSCE.
 - (18) O. Kiyomiya, S. Nakayama and H. Tsuchida (1975), "Observations of Dynamic Response of Kinuura Submerged Tunnel during Earthquakes and Dynamic Response Analysis (in Japanese)", Technical Note of the Port and Harbour Research Institute, Ministry of Transport, No. 221.
 - (19) O. Kiyomiya and T. Fujisawa (1979), "Observations of Dynamic Response of Kinuura Submerged Tunnel during Earthquakes (in Japanese)", Proceedings of the 14th JSSMFE.
 - (20) Y. Hirai and H. Oishi (1978), "Findings of Seismic Observation of the Ohgishima Submerged Tunnel (in Japanese)", Technical Report of Nippon Kokan, No. 77.
 - (21) N. Nasu, J. Morioka and H. Oishi (1980), "Earthquake Observation and Strain Measurement in a Submarine Tunnel", the 7th WCEE.
 - (22) S. Goto, T. Katayama and K. Koyama (1980), "Comparison of Observed Data with Calculated Results by Dynamic Analysis of Embedded Storage Tank for LNG during Earthquakes (in Japanese)", Preprint of the 35th Annual Meeting, JSCE.
 - (23) K. Kurahashi, S. Goto and K. Koyama (1980), "Observation of Embedded Storage Tank for LNG during Earthquakes (in Japanese)", Preprint of the 35th Annual Meeting, JSCE.
 - (24) K. Kubo et al. (1980), "Study on Dynamic Behaviors of Ground and Underground Structure (in Japanese)", Science Foundation by the Ministry of Education, No. A-55-2.
 - (25) Kanagawa Water Supply Authority (1980), "Observation and Analysis of Dynamic Behavior of Buried Pipeline during Earthquakes".
 - (26) Earthquake Resistant Guidance for Water Supply Facilities, JWWA (1979).
 - (27) M. Nakamura and B. Hashimoto (1980), "A Simple Method of Calculation to Estimate Strains in Ground during Earthquake by Theory of Elastic Wave Propagation (in Japanese)", Bulletin of Science and Engineering Research Laboratory, Waseda University, No. 92.
 - (28) M. Nakamura, T. Katayama and K. Kubo (1980), "A Simple Method of Calculation to Estimate Strains in Ground during Earthquake by Theory of Elastic Wave Propagation (in Japanese)", Preprint of the 35th Annual Meeting, JSCE.
 - (29) M. Nakamura, T. Katayama and K. Kubo (1980), "An Engineering Method to Estimate Strains in Ground during Earthquakes (in Japanese)", Preprint of the 30th Applied Mechanics Annual Meeting.

NOTATION

- A ; Acceleration amplitude used in the Technical Guidance for Petroleum Pipeline (cm/sec²)
 a ; Measured peak ground acceleration (cm/sec²)
 a_x, a_y, a_z ; Measured peak acceleration of a pipeline in the x , y and z direction, respectively (cm/sec²)
 C ; a_x/A
 D ; Pipe diameter (cm)
 E ; Young's modulus of pipe (kg/cm²)
 e ; Calculated strain
 e_B ; Ground strain corresponding to $K_{Oh}=1$ that causes bending strain in pipe
 e_{Bmax} ; Maximum of e_B ($\phi=0$)
 e_{CG} ; Axial strain $C \cdot e_{Lmax}$ of ground calculated by the Technical Guidance
 e_{CL} ; Axial strain $C \cdot \alpha_1 \cdot e_{Lmax}$ of pipe calculated by the Technical Guidance
 e_{CT} ; Compound strain $C \cdot e_T$ of pipe calculated by the Technical Guidance
 e_L ; Ground strain in axial direction of pipeline
 e_{Lmax} ; Maximum of e_L ($\phi=\pi/4$)
 e_P ; Ground strain calculated by the authors' method
 e_T ; Compound strain of pipe calculated by the Technical Guidance
 H_i ; Thickness of the i -th layer (cm)
 I ; Moment of inertia of pipe (cm⁴)
 K_1 ; Force per unit surface area of pipe that produces a unit of relative axial displacement between pipe and soil (kg/cm²)
 K_2 ; Force per unit surface area of pipe that produces a unit of relative lateral displacement between pipe and soil (kg/cm²)
 K_{Oh} ; Seismic coefficient at the design foundation
 L ; Wave length (cm)
 M ; Earthquake magnitude
 N ; Number of data
 S ; Cross-sectional area of pipe (cm²)
 S_V ; Response velocity at the ground surface for $K_{Oh}=1$ (cm/sec)
 T ; Natural period of ground (sec)
 U ; Horizontal displacement amplitude at ground surface (cm)
 U_B ; Displacement amplitude of ground in y -direction (cm)
 U_L ; Displacement amplitude of ground in x -direction (cm)
 V_{si} ; Shear wave velocity of the i -th layer (cm/sec)
 v_x, v_y ; Peak velocities of pipeline in x and y direction, respectively (cm/sec)
 x ; Axis along buried pipeline
 x' ; Direction of wave propagation
 y ; Axis perpendicular to x axis
 z ; Vertical axis
 α_1 ; Factor of transmission of axial strain from soil to pipe
 α_2 ; Factor of transmission of bending strain from soil to pipe

γ ; Coefficient of correlation
 Δ ; Epicentral distance (km)
 ϵ ; Measured strain
 ϵ_L ; Measured axial strain
 ρ ; Radius of curvature of pipe (cm)
 σ ; Standard deviation about regression line
 ϕ ; Angle between the pipeline axis and the direction of earthquake wave propagation (radian)

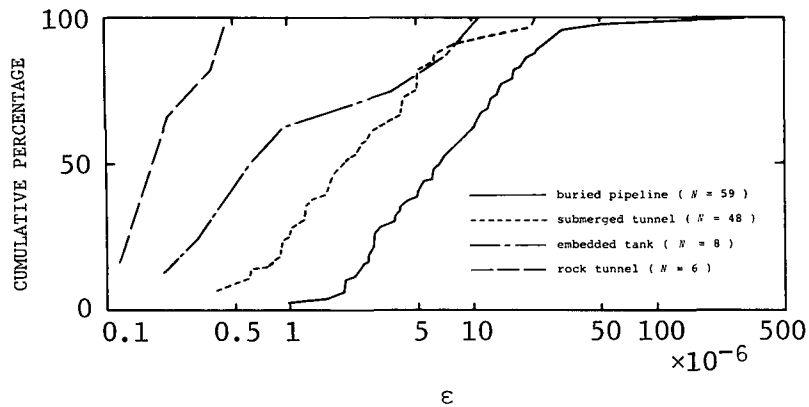


Fig. 1. Cumulative Frequency Distribution Curves for ϵ

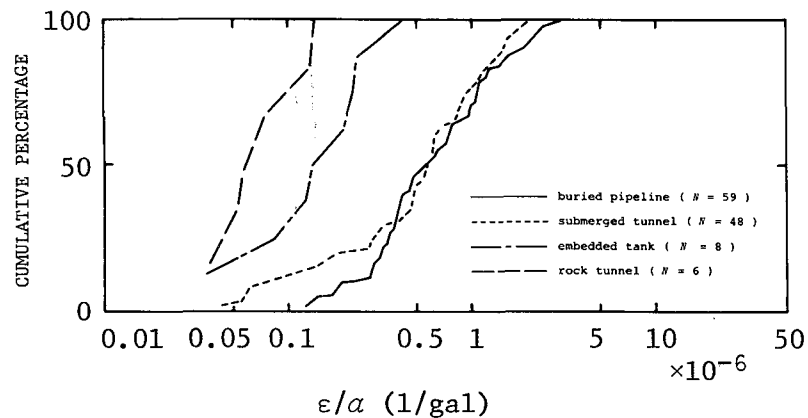


Fig. 2. Cumulative Frequency Distribution Curves for ϵ/a

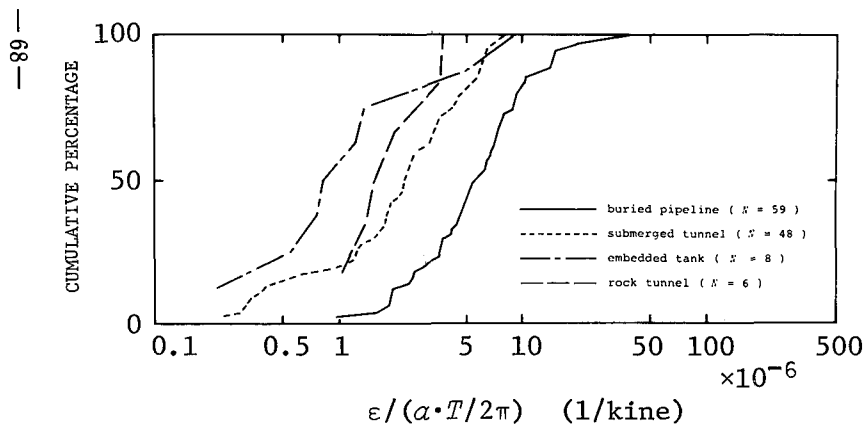


Fig. 3. Cumulative Frequency Distribution Curves for $\epsilon/(\alpha \cdot T/2\pi)$

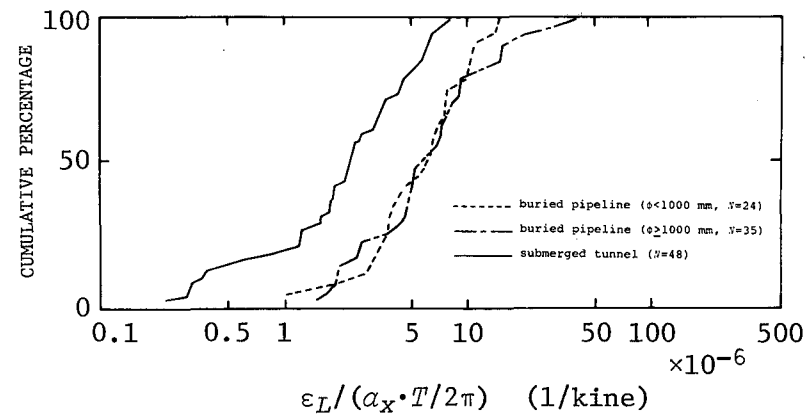


Fig. 4. Cumulative Frequency Distribution Curves for $\epsilon_L/(\alpha_x \cdot T/2\pi)$ (Submerged Tunnels and Buried Pipelines with $D < 1000$ and $D \geq 1000$)

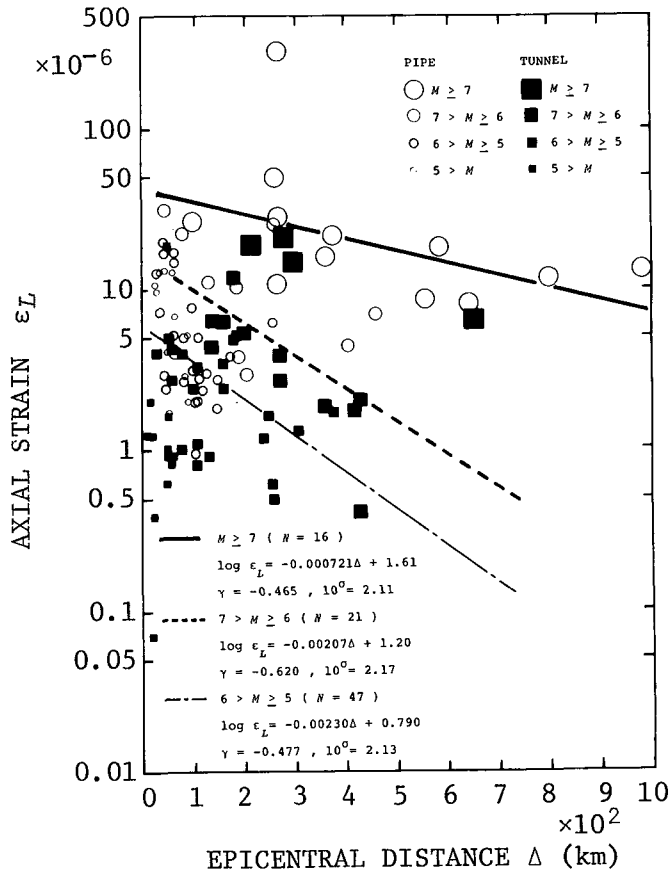


Fig.5. Relation between Axial Strain and Epicentral Distance for Linear Underground Structures

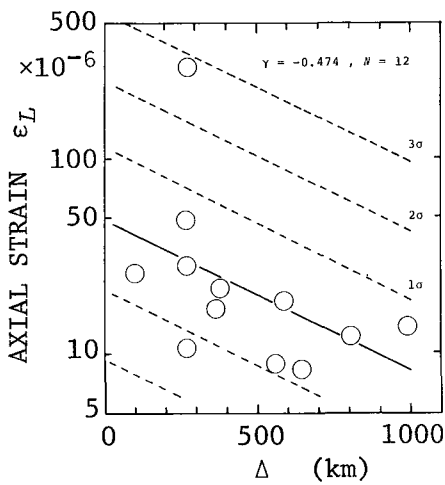


Fig.6. Relation between Axial Pipe Strain and Epicentral Distance ($M > 7$)

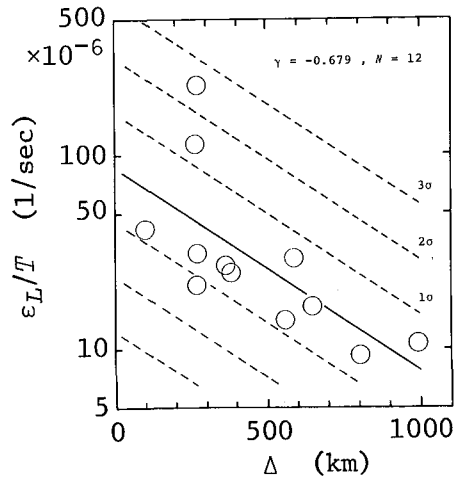


Fig.7. Relation between ϵ_L/T and Epicentral Distance for Pipelines ($M > 7$)

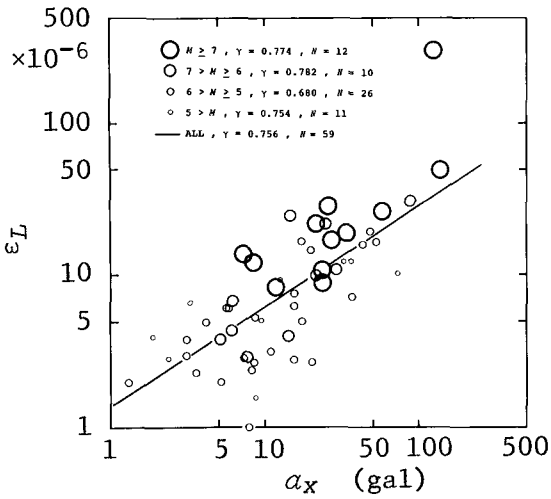


Fig. 8. Relation between Axial Pipe Strain and Longitudinal Peak Acceleration

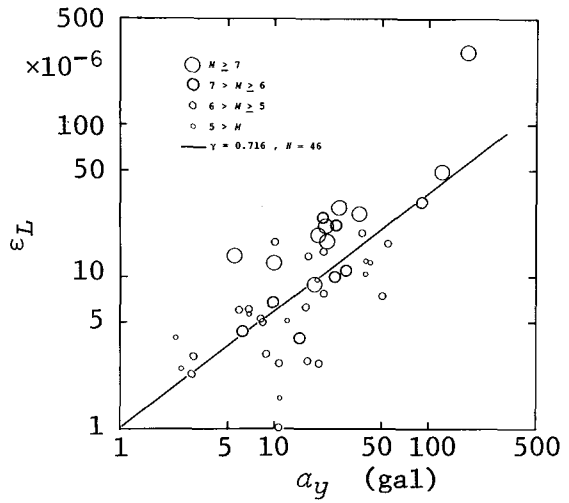


Fig. 9. Relation between Axial Pipe Strain and Lateral Peak Acceleration

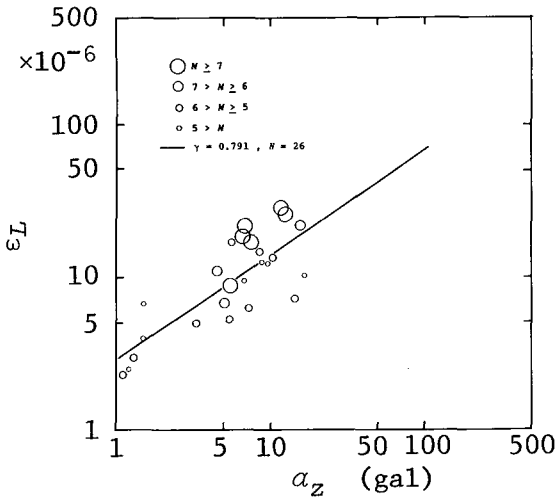


Fig. 10. Relation between Axial Pipe Strain and Vertical Peak Acceleration

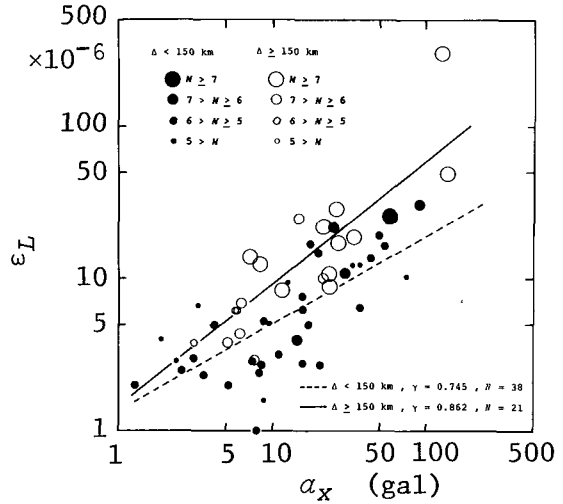


Fig. 11. Relation between Axial Pipe Strain and Longitudinal Peak Acceleration ($\Delta < 150$ km and $\Delta \geq 150$ km)

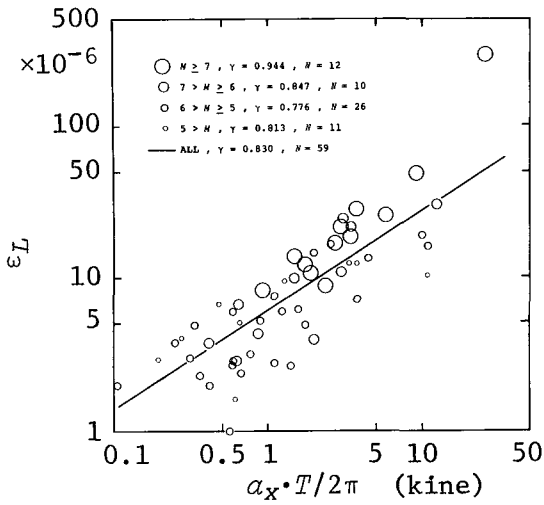


Fig.12. Relation between Axial Pipe Strain and $\alpha_x \cdot T / 2\pi$

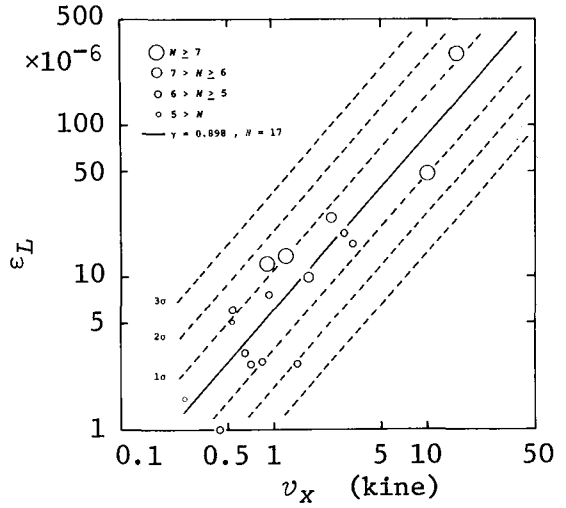


Fig.13. Relation between Axial Pipe Strain and Peak Velocity v_x

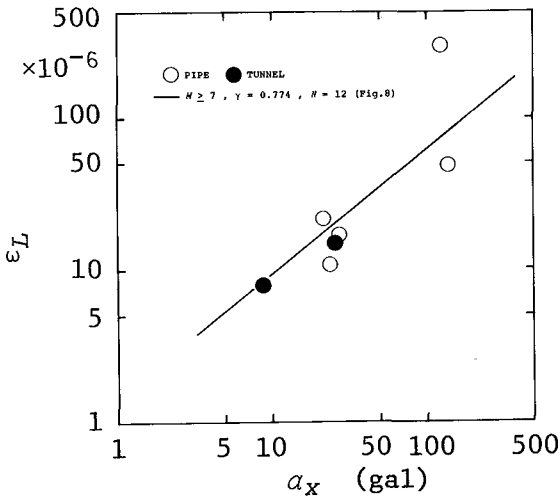


Fig.14. Observed Axial Strain in Linear Structures and Longitudinal Peak Acceleration α_x during the Miyagi-ken-oki Earthquake

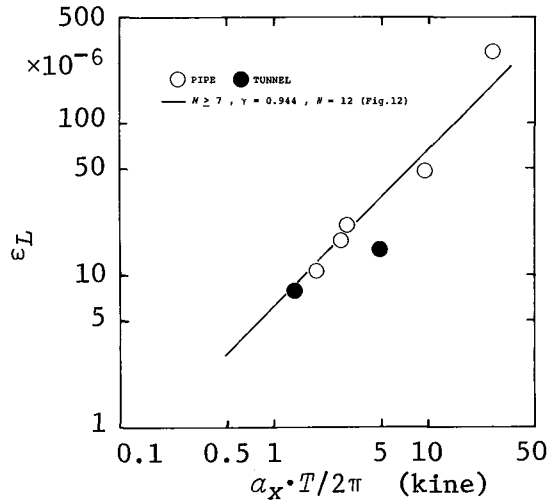


Fig.15. Observed Axial Strain in Linear Structures versus $\alpha_x \cdot T / 2\pi$ for the Data Obtained from the Miyagi-ken-oki Earthquake

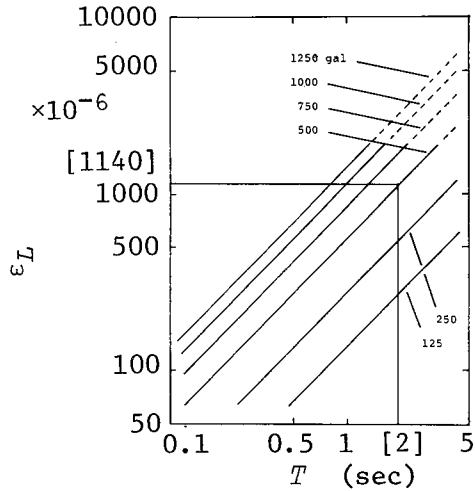


Fig. 16. Relation between ϵ_L and T for Various Levels of a_x Obtained by the Regression Equation ($M > 7$) in Fig. 12.

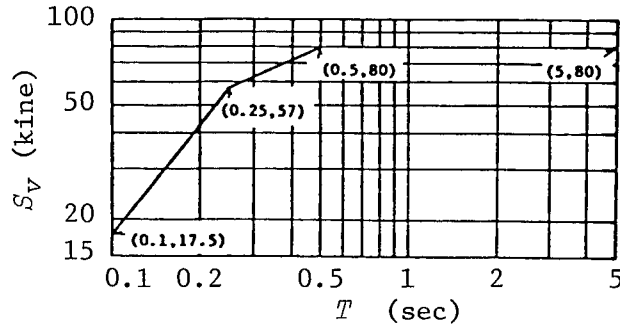


Fig. 18. Design Velocity Response Spectrum for Motion with Peak Acceleration 1 g (Technical Guidance for Petroleum Pipeline)

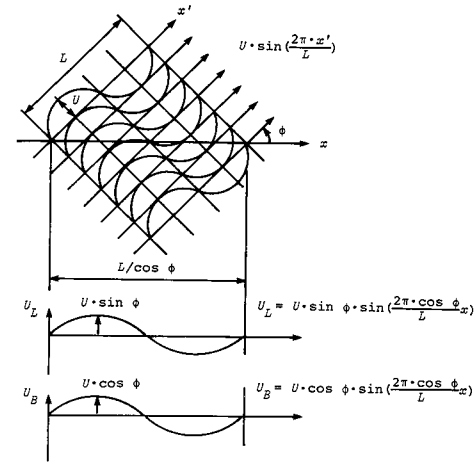


Fig. 17. Concept of Pipeline Design for Propagating Seismic Waves

- 1 Determine S_v for T at the Site from Fig. 18
- 2 Compute U by Eq. (13) by Assuming that $K_{oh} = 1$
- 3 Compute e_{Lmax} , $\alpha_1 \cdot e_{Lmax}$, e_T by Eqs. (8) and (12)
- 4 Convert U to A by $A = (2\pi/T)^2 U$
- 5 $C = \alpha_x / A$ where $\alpha_x =$ Measured Peak Acceleration
- 6 Obtain Strains by the Technical Guidance for Petroleum Pipeline by Using
 $e_{CG} = C \cdot e_{Lmax}$, $e_{CL} = C \cdot \alpha_1 \cdot e_{Lmax}$, $e_{CT} = C \cdot e_T$
- 7 Compare Measured Strains ϵ_L with Computed Strains Obtained in Box 6

Fig. 19. Flow Chart of Comparison between Observed and Calculated Strains

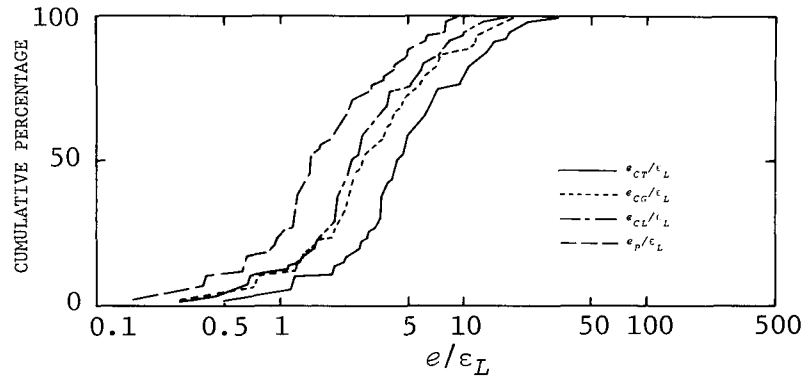


Fig. 20. Cumulative Frequency Distributions of e/ϵ_L
(= Calculated/Measured)

Table 1. Observation Sites and Types of Underground Structures

NO.	SITE	STRUCTURE	T (SEC)	DIAMETER (MM)	THICKNESS (MM)
1	YOKOHAMA	PIPE	0.914	165.2	5.0
2	SOOKA	PIPE	0.644	406.4	7.9
3	ODMORI	PIPE	0.632	216.3	5.8
4	KANSEN	PIPE	0.437	1554.0	18.0
5	SHIMONAGA	PIPE	1.310	1041.0	13.0
6	HACHINOHE	PIPE	0.504	1219.2	16.0
7	MINAMIWATARIDA	PIPE	0.878	1838.0	19.0
8	HANEDA	TUNNEL	1.600	--	--
9	KINUURA	TUNNEL	0.969	--	--
10	OOGISHIMA	TUNNEL	1.220	--	--
11	NEGISHI	TANK	0.294	--	--
12	SHIMIZU	TANK	1.020	--	--
13	ISHIZUKAYAMA	ROCK TUNNEL	0.229	--	--

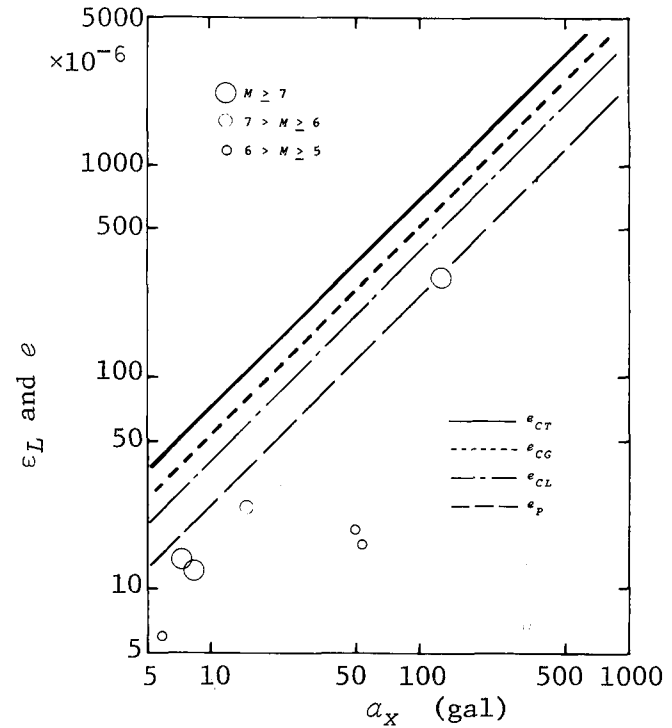


Fig. 21. Various Calculated Strains and Observed Strains for the Data Recorded at the Shimonaga Site

Table 2. List of Earthquakes

NO.	DATE	EPICENTER N E		DEPTH (KM)	MAGNITUDE
1	1970 9 14	38.68	142.33	40.	6.2
2	1970 9 30	35.48	139.63	40.	4.8
3	1972 1 4	35.87	140.53	40.	5.0
4	1972 1 27	35.68	139.12	40.	4.8
5	1972 8 31	35.88	136.77	10.	6.0
6	1972 9 25	38.35	142.07	50.	5.5
7	1972 10 6	34.40	138.52	30.	5.5
8	1972 11 5	—	—	50.	5.5
9	1972 11 6	36.20	139.80	40.	5.1
10	1972 12 4	33.20	141.08	50.	7.3
11	1972 12 8	35.58	140.00	90.	4.8
12	1973 1 17	—	—	60.	4.1
13	1973 1 21	36.05	139.87	70.	4.8
14	1973 2 10	33.35	140.72	30.	5.1
15	1973 3 17	36.95	141.68	50.	5.3
16	1973 3 27	35.52	139.93	60.	4.9
17	1973 4 25	33.53	140.87	50.	5.5
18	1973 8 24	36.52	139.75	110.	5.0
19	1973 9 30	35.65	140.67	50.	5.9
20	1973 10 1	35.62	140.80	60.	5.8
21	1973 11 19	38.88	142.15	50.	6.4
22	1973 11 25	33.85	135.42	60.	5.9
23	1973 11 25	33.88	135.38	60.	5.8
24	1973 12 22	35.22	140.28	70.	5.0
25	1974 2 10	35.03	136.93	40.	5.3
26	1974 2 22	33.13	137.12	400.	6.9
27	1974 3 3	35.08	140.15	40.	6.0
28	1974 5 5	37.75	141.85	40.	5.5
29	1974 5 9	34.57	138.80	10.	6.9
30	1974 6 27	33.75	139.20	10.	6.1
31	1974 7 8	36.42	141.20	40.	6.3
32	1974 8 4	36.02	139.92	50.	5.8
33	1974 8 16	35.25	136.18	50.	4.9
34	1974 9 27	33.72	141.55	60.	6.4
35	1974 10 9	36.05	139.92	60.	4.8
36	1974 10 29	35.60	140.33	70.	4.9
37	1974 10 31	36.10	139.95	60.	4.6
38	1974 11 1	35.60	140.33	60.	4.3
39	1974 11 16	35.60	140.33	40.	6.1
40	1974 11 21	35.62	140.33	60.	4.7
41	1974 11 30	30.60	138.27	420.	7.6
42	1975 1 14	35.25	141.22	30.	5.1
43	1975 1 21	34.98	141.35	30.	5.9
44	1975 2 8	35.82	140.12	460.	5.4
45	1975 3 11	36.52	139.72	130.	5.1
46	1975 3 14	35.30	136.83	50.	5.3

NO.	DATE	EPICENTER N E		DEPTH (KM)	MAGNITUDE
47	1975 4 12	36.17	140.02	50.	4.0
48	1975 4 18	36.13	139.85	50.	5.0
49	1975 6 16	40.13	142.25	30.	4.9
50	1975 6 18	40.16	142.43	40.	5.0
51	1975 6 18	40.87	143.25	30.	5.5
52	1975 8 12	31.70	138.30	360.	6.9
53	1975 9 20	—	—	50.	5.9
54	1975 10 30	41.95	142.78	60.	6.0
55	1975 12 15	35.50	140.20	60.	4.6
56	1976 3 15	40.97	141.97	60.	4.3
57	1976 5 13	35.70	139.80	40.	4.2
58	1976 6 2	41.45	142.03	60.	5.0
59	1976 6 16	35.52	139.00	20.	4.7
60	1976 6 16	35.50	139.00	20.	5.5
61	1976 7 8	40.23	142.43	30.	5.9
62	1976 8 18	34.77	138.93	0.	5.5
63	1976 12 29	36.80	139.20	140.	5.8
64	1977 2 4	35.08	138.28	10.	4.2
65	1977 2 18	41.45	141.97	60.	5.4
66	1977 4 25	40.08	142.68	30.	5.0
67	1977 6 4	35.52	140.05	60.	4.6
68	1977 9 28	—	—	60.	4.8
69	1977 10 5	36.13	139.87	60.	5.4
70	1977 12 17	36.58	141.08	50.	5.6
71	1978 1 14	34.77	139.25	10.	7.0
72	1978 1 15	34.83	138.88	20.	5.8
73	1978 1 15	34.80	138.83	10.	5.4
74	1978 2 20	38.20	142.70	50.	6.7
75	1978 3 7	31.60	137.80	440.	7.8
76	1978 3 20	36.10	139.90	60.	5.5
77	1978 3 25	44.33	149.82	40.	7.3
78	1978 4 7	35.20	141.10	40.	5.7
79	1978 5 15	40.20	142.50	40.	5.0
80	1978 5 16	40.95	141.47	10.	5.8
81	1978 5 16	40.93	141.45	10.	5.8
82	1978 6 12	38.15	142.22	30.	7.4
83	1978 6 12	38.20	142.39	40.	5.8
84	1978 6 12	—	—	—	—
85	1978 6 14	38.35	142.48	40.	6.3
86	1978 6 21	38.25	142.00	50.	5.8
87	1978 12 6	—	—	100.	7.7
88	1980 6 29	34.92	139.23	10.	6.7
89	1980 9 24	36.10	139.70	60.	6.0
90	1980 9 25	35.50	140.20	70.	6.1
91	1978 4 7	35.00	141.05	40.	—

Table 3. Summary of Observed Data

DATA NO.	SITE NO.	EARTHQUAKE NO.	MAGNITUDE	EPICENTRAL DISTANCE (KM)	ACCELERATION (GAL)			VELOCITY (KINE)		STRAIN * (MICRO)	
					X	Y	Z	X	Y	STRAIN1	STRAIN2
1	1	8	3.5	50.	1.9	2.3	1.5	1.0	1.0	4.00	1.0
2	1	9	5.1	65.	17.5	10.0	5.6	1.0	1.0	17.00	1.0
3	1	10	7.3	270.	26.0	26.0	11.5	1.0	1.0	28.40	1.0
4	1	12	4.1	60.	3.3	6.8	1.5	1.0	1.0	12.30	1.0
5	1	13	4.8	65.	3.3	6.8	1.5	1.0	1.0	6.70	1.0
6	1	16	4.9	26.	73.7	38.8	16.5	1.0	1.0	10.30	1.0
7	2	37	4.6	35.	32.9	41.5	9.6	1.0	1.0	12.30	0.70
8	2	39	6.1	130.	29.5	29.0	4.5	1.0	1.0	11.00	3.80
9	2	41	7.6	588.	33.8	19.0	6.6	1.0	1.0	18.70	4.20
10	2	44	5.4	28.	43.8	16.4	10.2	1.0	1.0	13.60	3.90
11	2	47	4.0	44.	36.7	39.0	8.8	1.0	1.0	12.50	4.50
12	2	48	5.0	36.	37.0	49.5	14.3	1.0	1.0	7.30	2.80
13	2	52	6.9	460.	6.3	9.7	5.0	1.0	1.0	6.80	2.30
14	3	63	5.8	146.	15.5	15.9	7.2	1.0	1.0	6.30	1.0
15	3	67	4.6	29.	12.6	18.9	6.7	1.0	1.0	9.50	1.0
16	3	69	5.4	66.	19.8	20.5	8.5	1.0	1.0	14.70	1.0
17	3	70	5.6	167.	5.9	6.8	4.7	1.0	1.0	6.10	1.0
18	3	71	7.0	100.	57.9	35.3	12.3	1.0	1.0	26.10	1.0
19	3	72	5.8	114.	17.3	8.4	3.3	1.0	1.0	5.00	1.0
20	3	73	5.4	120.	3.6	2.9	1.1	1.0	1.0	2.30	1.0
21	3	75	7.8	559.	23.4	18.1	5.5	1.0	1.0	8.90	1.0
22	3	76	5.5	63.	8.8	8.2	5.4	1.0	1.0	5.30	1.0
23	3	78	5.7	129.	3.1	3.0	1.3	1.0	1.0	3.00	1.0
24	3	91	***	140.	2.6	2.5	1.2	1.0	1.0	2.50	1.0
25	3	82	7.4	365.	27.0	21.7	7.5	1.0	1.0	17.00	1.0
26	4	49	4.9	89.	9.5	12.1	0.53	0.73	1.0	5.10	1.0
27	4	50	5.0	99.	15.6	20.6	0.91	1.10	1.0	7.70	1.0
28	4	51	5.5	148.	8.5	10.5	0.70	0.58	1.0	2.70	1.0
29	4	54	6.0	184.	21.4	24.4	1.66	1.61	1.0	10.00	1.0
30	4	56	4.3	56.	8.8	10.7	0.26	0.27	1.0	1.60	1.0
31	4	58	5.0	105.	8.0	10.4	0.44	0.62	1.0	0.96	1.0
32	4	61	5.9	85.	20.3	19.3	1.41	1.20	1.0	2.70	1.0
33	4	65	5.4	114.	15.7	16.2	0.83	0.79	1.0	2.80	1.0
34	4	66	5.0	108.	11.1	8.8	0.64	0.53	1.0	3.20	1.0
35	4	82	7.4	265.	137.5	120.9	9.70	7.70	1.0	48.90	1.0
36	5	75	7.8	992.	7.2	5.5	1.18	0.78	1.0	13.90	1.0
37	5	77	7.3	805.	8.3	9.8	0.90	1.06	1.0	12.20	1.0
38	5	80	5.8	45.	52.8	54.7	3.22	3.95	1.0	16.50	1.0
39	5	81	5.8	44.	48.6	36.5	2.84	2.80	1.0	19.40	1.0
40	5	82	7.4	272.	125.1	178.8	15.00	12.00	1.0	299.20	1.0
41	5	85	6.3	258.	14.8	20.5	2.33	3.24	1.0	24.80	1.0
42	5	86	5.8	258.	5.9	5.9	0.53	0.71	1.0	6.10	1.0
43	6	49	4.9	87.	2.4	1.0	1.0	1.0	1.0	2.90	1.0
44	6	51	5.5	150.	0.6	1.0	1.0	1.0	1.0	1.80	1.0
45	6	53	5.9	176.	3.1	1.0	1.0	1.0	1.0	3.80	1.0
46	6	54	6.0	190.	5.2	1.0	1.0	1.0	1.0	3.80	1.0
47	6	58	5.0	111.	1.3	1.0	1.0	1.0	1.0	2.00	1.0
48	6	61	5.9	84.	4.2	1.0	1.0	1.0	1.0	5.00	1.0
49	6	65	5.4	109.	5.2	1.0	1.0	1.0	1.0	2.00	1.0
50	6	68	4.8	91.	0.9	1.0	1.0	1.0	1.0	2.00	1.0
51	6	74	6.7	205.	7.8	1.0	1.0	1.0	1.0	2.90	1.0
52	6	80	5.8	48.	8.3	1.0	1.0	1.0	1.0	2.40	1.0
53	6	81	5.8	46.	7.4	1.0	1.0	1.0	1.0	2.90	1.0
54	6	82	7.4	269.	23.4	1.0	1.0	1.0	1.0	10.70	1.0
55	6	87	7.7	646.	11.5	1.0	1.0	1.0	1.0	8.40	1.0
56	7	74	6.7	406.	6.2	7.4	1.0	1.0	1.0	4.35	1.0
57	7	82	7.4	379.	21.4	28.0	6.8	1.0	1.0	21.80	1.0
58	7	88	6.7	78.	25.0	26.7	15.5	1.0	1.0	22.00	1.0
59	7	89	6.0	67.	14.4	19.5	1.0	1.0	1.0	4.00	1.0
60	7	90	6.1	44.	90.0	71.0	1.0	1.0	1.0	31.00	1.0

*

	PIPE	TUNNEL	TANK	ROCK TUNNEL
STRAIN1	LONGITUDINAL AXIAL STRAIN ϵ_L	LONGITUDINAL AXIAL STRAIN ϵ_L	HORIZONTAL CIRCUMFERENTIAL STRAIN	LONGITUDINAL AXIAL STRAIN
STRAIN2	CIRCUMFERENTIAL STRAIN	BENDING STRAIN	VERTICAL AXIAL STRAIN	—————

Table 3. Summary of Observed Data (Continued)

DATA NO.	SITE NO.	EARTHQUAKE NO.	MAGNITUDE	EPICENTRAL DISTANCE (KM)	ACCELERATION (GAL)			VELOCITY (KINE)		STRAIN (MICRO)	
					X	Y	Z	X	Y	STRAIN1	STRAIN2
61	8	1	6.2	420.	2.6	12.1	1.8	1.70			
62	8	2	4.8	12.	12.1	1.8	1.70				
63	8	3	5.0	80.	6.8	2.3	1.6	1.00			
64	8	4	4.8	60.	6.8	2.3	1.6	0.80			
65	8	5	6.0	270.	2.3	10.9	1.6	2.60			
66	8	6	5.5	380.	1.6	10.9	1.6	1.70			
67	8	7	5.5	160.	10.9	14.7	10.9	3.50			
68	8	10	7.3	280.	14.7	15.0	14.7	20.90			
69	8	11	4.8	20.	15.0	2.7	0.9	1.20			
70	8	13	4.8	55.	2.7	0.9	0.6	1.60			
71	8	14	5.1	260.	0.9	0.6	13.6	0.50			
72	8	15	5.3	240.	0.6	1.2	1.2	1.20			
73	8	16	4.9	17.	13.6	1.2	1.9	2.00			
74	8	17	5.5	250.	1.2	1.9	4.5	1.60			
75	8	18	5.0	110.	1.9	4.5	4.5	1.10			
76	8	19	5.9	80.	4.5	4.5	4.5	4.00			
77	8	20	5.8	100.	4.5	1.8	6.9	2.40			
78	8	21	6.4	430.	1.8	6.9	3.8	2.00			
79	8	24	5.0	60.	6.9	5.1	5.1	4.20			
80	8	26	6.9	360.	3.8	0.9	0.9	1.80			
81	8	27	6.0	135.	5.1	0.9	0.9	4.20			
82	8	28	5.5	310.	0.9	9.3	2.9	1.30			
83	8	29	6.9	190.	9.3	2.9	3.8	11.60			
84	8	30	6.1	200.	2.9	3.8	11.0	5.20			
85	8	31	6.3	160.	3.8	11.0	7.8	6.10			
86	8	32	5.8	55.	11.0	7.8	2.0	5.00			
87	8	34	6.4	270.	7.8	2.0	2.4	4.80			
88	8	35	4.8	60.	2.0	2.4	2.1	0.90			
89	8	36	4.9	50.	2.4	2.1	9.0	1.00			
90	8	38	4.3	50.	2.1	9.0	2.0	0.60			
91	8	39	6.1	140.	9.0	2.0	0.4	6.10			
92	8	40	4.7	50.	2.0	0.4	10.3	0.90			
93	8	42	5.1	135.	1.0	10.3	26.9	0.90			
94	8	43	5.9	160.	2.8	13.1	71.2	2.40			
95	8	44	5.4	60.	8.8	13.1	24.0	2.70			
96	8	45	5.1	110.	2.0	13.1	24.0	0.80			
97	8	46	5.3	260.	0.4	18.6	22.1	0.60			
98	9	22	5.9	185.	10.3	18.6	8.7	5.00			
99	9	23	5.8	185.	26.9	4.7	6.4	5.00			
100	9	25	5.3	30.	71.2	4.7	6.4	4.00			
101	9	33	4.9	50.	24.0	27.8	1.6	6.80			
102	9	71	7.0	215.	22.1	18.6	1.6	21.50			
103	9	82	7.4	655.	8.7	4.7	6.4	8.00			
104	10	52	6.9	430.	6.4	4.7	1.6	0.40	0.25		
105	10	55	4.6	25.	6.4	1.6	1.6	0.38	0.57		
106	10	57	4.2	22.	1.6	1.6	19.2	0.07			
107	10	60	5.5	110.	19.2	24.9	45.5	3.20	1.60		
108	10	82	7.4	300.	24.9	45.5	16.2	15.00	5.00		
109	11	71	7.0	70.	45.5	22.2	3.0	10.60	4.60		
110	11	82	7.4	370.	16.2	9.8	3.0	7.00	3.30		
111	12	39	6.1	260.	3.0	0.69	1.9	0.60			
112	12	41	7.6	540.	1.9	0.65	1.7	0.44			
113	12	59	4.7	70.	1.7	0.23	6.7	0.21			
114	12	60	5.5	70.	6.7	0.08	1.7	0.91			
115	12	62	5.5	50.	1.7	0.68	9.0	0.62			
116	12	64	4.2	35.	9.0	0.56	41.9	0.32			
117	12	71	7.0	80.	41.9	6.43	1.1	3.59			
118	13	79	5.0	120.	1.1	0.15	1.4	0.15			
119	13	80	5.8	190.	1.4	0.18	3.8	0.18			
120	13	83	5.8	120.	3.8	0.12	3.2	0.22			
121	13	84	5.8	120.	3.2	0.38	5.2	0.12			
122	13	85	6.3	110.	5.2	0.38	8.9	0.38			
123	13	86	5.8	105.	8.9	0.46		0.46			

Table 4. Summary of Regression Lines ($Y=\beta X+\alpha$)

Fig.	Condition	N	γ	Y	X	β	α	σ_Y	10^{σ_Y}
5	$M>7$	16	-0.465	$\log \epsilon_L$	Δ	-0.000721	1.61	0.325	2.11
5	$7>M>6$	21	-0.620	$\log \epsilon_L$	Δ	-0.00207	1.20	0.336	2.17
5	$6>M>5$	47	-0.477	$\log \epsilon_L$	Δ	-0.00230	0.790	0.328	2.13
6	—	12	-0.474	$\log \epsilon_L$	Δ	-0.000767	1.69	0.357	2.28
7	—	12	-0.679	$\log (\epsilon_L/T)$	Δ	-0.00105	1.94	0.283	1.92
8	—	59	0.756	$\log \epsilon_L$	$\log a_x$	0.661	0.139	0.287	1.94
8	$M>7$	12	0.774	$\log \epsilon_L$	$\log a_x$	0.808	0.171	0.257	1.81
8	$7>M>6$	10	0.782	$\log \epsilon_L$	$\log a_x$	0.756	0.0554	0.222	1.67
8	$6>M>5$	26	0.680	$\log \epsilon_L$	$\log a_x$	0.500	0.177	0.248	1.77
8	$5>M$	11	0.754	$\log \epsilon_L$	$\log a_x$	0.403	0.349	0.204	1.60
9	—	46	0.716	$\log \epsilon_L$	$\log a_y$	0.771	0.0147	0.305	2.02
10	—	26	0.791	$\log \epsilon_L$	$\log a_z$	0.689	0.459	0.185	1.53
11	$\Delta \geq 150$	21	0.862	$\log \epsilon_L$	$\log a_x$	0.796	0.171	0.240	1.74
11	$\Delta < 150$	38	0.745	$\log \epsilon_L$	$\log a_x$	0.570	0.137	0.253	1.79
12	—	59	0.830	$\log \epsilon_L$	$\log (a_x \cdot T/2\pi)$	0.652	0.789	0.245	1.76
12	$M>7$	12	0.944	$\log \epsilon_L$	$\log (a_x \cdot T/2\pi)$	1.02	0.804	0.134	1.36
12	$7>M>6$	10	0.847	$\log \epsilon_L$	$\log (a_x \cdot T/2\pi)$	0.706	0.780	0.189	1.55
12	$6>M>5$	26	0.776	$\log \epsilon_L$	$\log (a_x \cdot T/2\pi)$	0.494	0.685	0.213	1.63
12	$5>M$	11	0.813	$\log \epsilon_L$	$\log (a_x \cdot T/2\pi)$	0.412	0.753	0.181	1.52
13	—	17	0.898	$\log \epsilon_L$	$\log v_x$	1.16	0.791	0.259	1.82

Table 5. Comparison of Observed Strains and Various Calculated Strains (Shimonaga Site)

M	$\epsilon_L (\times 10^{-6})$	a_x (gal)	e_P/ϵ_L	e_{CL}/ϵ_L	e_{CG}/ϵ_L	e_{CT}/ϵ_L
7.4	299	125	1.0	1.7	2.2	3.0
$M>7$	13.9	7.2	1.3	2.1	2.7	3.7
7.3	12.2	8.3	1.7	2.8	3.6	4.9
6.3	24.8	14.8	1.5	2.4	3.1	4.3
5.8	6.1	5.9	2.4	4.0	5.1	7.0
5.8	19.4	48.6	6.1	10.2	13.2	17.9
5.8	16.5	52.8	7.8	13.0	16.8	22.8